A CONTEXT-APPROPRIATE APPROACH TO MARINE ^{14}C CALIBRATION: ΔR AND BAYESIAN FRAMEWORK FOR THE NUVUK CEMETERY, POINT BARROW, ALASKA

Anthony Krus[1,2]
Anne M. Jensen[3]
W. Derek Hamilton[1]
Kerry Sayle[1]

Author Affiliations

[1]University of Glasgow, SUERC, Scottish Enterprise Technology Park, Rankine Avenue East Kilbride G75 0QF, Scotland, United Kingdom. Corresponding author. Email: tony.krus@glasgow.ac.uk

[2]Department of Anthropology and Sociology, University of South Dakota, Vermillion, SD, 57069

[3]University of Alaska Fairbanks, Department of Anthropology, PO Box 757720, Fairbanks AK 99775-7720

ABSTRACT

This study provides an assessment of the temporal changes in ΔR, which is the local deviation from the global surface water Marine Reservoir Effect (MRE), in the Point Barrow area of the Alaskan Arctic, a coastal archaeological area that has experienced severe erosion accelerated by global warming. A total of 26 samples were submitted for radiocarbon (^{14}C) dating from eight secure Thule (AD 1000–1750) archaeological contexts, and specifically from archaeological features with paired processed seal and caribou bones that had been frozen *in situ*. This new approach towards ΔR estimation provides a best-fit local correction for the ^{14}C dating of human populations by focusing on the marine mammal (seals) predominantly consumed by the Thule (Coltrain et al. 2016). The weighted-mean ΔR value on these pairs is 450 ± 84 years, which is about 50 years less than the weighted-mean (506 ± 69 years) for the Point Barrow area calculated through ^{14}C measurements from four known-age bivalves collected in AD 1913 (McNeely et al. 2006). The effects of using this new ΔR value for calibration was assessed through the Bayesian chronological modeling of 54 ^{14}C measurements from samples of human skeletons interred in the Nuvuk cemetery at Point Barrow, the largest ancient cemetery in northwest Alaska and traditionally thought to date to the Thule and earlier Birnirk (AD 500–1000) periods.

KEYWORDS

^{14}C calibration; Marine reservoir effect; Nuvuk; Point Barrow, AK; Bayesian modeling; Birnirk period; Thule period; Chronology

INTRODUCTION

Approximately one thousand years ago, during the Medieval Climate Anomaly (AD 950–1250), the Thule spread throughout the American Arctic and 'replaced' the existing Paleo-Eskimo populations. This represented the final ancient human migration into the American Arctic (Raghavan et al. 2014). While earlier Paleo-Eskimo groups were predominantly seasonally mobile foragers, the Thule established networks of sedentary villages strategically placed in prime locations to hunt seal, whale, and avian populations. Thule success in these challenging environments has long been attributed to their effective means for transportation, specifically dog sleds and large skin boats, and their sophisticated harpoon float gear for hunting large whales (Maxwell 1985; McGhee 1996).

The recent resurgence of radiocarbon (^{14}C) dating in Arctic archaeology has revealed that the Point Barrow area at the northernmost tip of Alaska played a pivotal role in Thule emergence and later served as the origin point for Thule migrations into the eastern Arctic (Jensen 2009a, 2009b; McGhee 2009; Morrison 2009). Thus far, 238 ^{14}C measurements have been obtained on archaeological samples from this area; primarily from marine mammals, driftwood, and human skeletal remains.

Conversely, the level of chronological precision that has been achieved for the interpretation of this data has been quite coarse, because almost all of the ^{14}C dated samples are either potentially residual or contain significant portions of marine-derived carbon (Jensen 2009a, 2009b; 2014). Arctic MRE offsets can vary from several hundred to over a thousand years, depending on the extended residence time of ^{14}C in local oceanic environments (McNeely et al. 2006), which presents a challenge for producing accurate ^{14}C calibrations. Point Barrow is located at the confluence of the Chukchi Sea and the Beaufort Sea, further complicating the issue due to marine creatures living in and across these two bodies of water.

ΔR values provide a local offset from the global MRE for surface waters (Queiroz-Alves et al. 2018). In the case of Point Barrow, the ΔR value traditionally used for interpretation (506 ± 69 years) is a weighted-mean of four values which have been calculated by dating known-age bivalves collected in 1913 from Point Barrow, the only ΔR values currently available for this study area (McNeely et al. 2006). While these early 20th century MRE values are normally applied to correct offsets from the Point Barrow area, it is questionable how reflective more recent values are of those from the past. Changes in upwelling, climate, and ocean currents will inevitably result in changes in local MRE values through time (Russell et al. 2010), and estimating ancient MRE values is a research topic that so far has been overlooked in the Alaskan Arctic.

Numerous contexts are available in the study area with contemporaneously deposited samples of marine- and terrestrial-derived carbon for ^{14}C dating, primarily from frozen *in situ* domestic Thule contexts with discarded, processed seals and caribou remains (Ford 1959; Stanford 1976; Hall and Fullerton 1990; Sheehan 1997; Jensen 2009a). This study has followed the multiple pair approach of Ascough et al. (2009) and Russell et al. (2010), whereby paired terrestrial and marine samples (e.g. seal bone and caribou bone) have been utilized to assess the ΔR value directly from animals consumed by the Thule population.

Previous analysis of $\delta^{13}C$ and $\delta^{15}N$ values from Thule skeletons interred in the Point Barrow region suggests that seals were the most significant food in Thule diets (Coltrain et al. 2016). Seals in Point Barrow regularly move throughout the coastal portions of the Chukchi Sea and Beaufort Sea during the open water season each year (Bengtson et al. 2005; Harwood et al. 2012; Lowry et al. 1998) and adult ring seals tend to be more territorial during the rest of the year (Crawford et al. 2012; Harwood et al. 2012; Kelly et al. 2010; Kraffit et al. 2007). The seal bones sampled for this project are all identified as likely ring seal (*Phoca hispida*) (Table 1) and so are likely to strongly reflect local marine reservoirs throughout the Chukchi Sea and Beaufort Sea. Thus, our ΔR for the Thule population is different than one based on measurements of sedentary marine organisms, which is not what local Thule communities were eating. Therefore, as it is derived directly from the foods that the Thule were eating, our suggested best-fit ΔR value based on paired samples of seal bone and caribou bone is more suitable for the correction of ^{14}C measurements from Point Barrow's human population.

This best-fit ΔR approach further allows for the correction and Bayesian modeling of ^{14}C data from human skeletons from the largest ancient cemetery in northwest Alaska (Nuvuk, Point Barrow). Advances in the statistical modeling of ^{14}C dates and archaeological data within a Bayesian framework is enabling researchers to better understand similar mortuary chronologies and even produce date estimates at generational-levels (Bayliss 2009; Bayliss et al. 2007; 2011).

METHODOLOGY

ΔR values, used to correct for local MRE ^{14}C offsets, were calculated using an analysis of multiple paired marine and terrestrial samples following the methods described in Russell (2011) and Russell et al. (2015). Twenty-six single-entity samples of paired caribou and seal bone were submitted for radiocarbon dating from eight secure archaeological contexts, specifically from contexts where such samples were frozen *in situ* (Table 1).

These samples were submitted to the Scottish Universities Environmental Research Centre (SUERC) to be measured by Accelerator Mass Spectrometry (AMS). Since the samples were well-preserved in the frozen Arctic environment, they were pretreated following the protocols for forensic bone described in Dunbar et al. (2016), where a lipid extraction process is employed prior to the standard collagen extraction method employed in the laboratory. Graphite targets were prepared and measured following Naysmith et al. (2010). SUERC maintains rigorous internal quality assurance procedures and participation in international inter-comparisons (Scott 2003; Scott et al. 2003; 2007; 2010), thus validating the measurement precision quoted for the ^{14}C ages. The C:N ratios suggest that bone preservation was sufficiently good to have confidence in the accuracy of the ^{14}C determinations (Table 1; Masters 1987; Tuross et al. 1988). Conventional ^{14}C ages (Stuiver and Polach 1977) are presented in Table 1, quoted according to the international standard set at the Trondheim Convention (Stuiver and Kra 1986). Calibrated date ranges were calculated using the relevant terrestrial or marine calibration curve of Reimer et al. (2013) and OxCal v4.3. Calibrations are cited in the text as 95% confidence intervals, with the end points rounded outwards to 10 years.

Carbon ($\delta\ ^{13}C$) and nitrogen ($\delta\ ^{15}N$) isotopic values were analyzed using a Thermo Scientific Delta V Advantage continuous-flow isotope ratio mass spectrometer (CF-IRMS) coupled via a Thermo Scientific ConfloIV to a Costech ECS 4010 elemental analyzer (EA) fitted with a pneumatic auto sampler. Samples were weighed into tin capsules (~600 μg) and combusted in the presence of oxygen in a single reactor containing tungstic oxide and copper wires at 1020°C to produce N_2 and CO_2. A magnesium perchlorate trap was used to eliminate water produced during the combustion process and the gases were separated in a 2 m stainless steel Porapak QS 50-80 mesh GC column heated to 70°C. Helium (100mL/min) was used as a carrier gas throughout the procedure. N_2 and CO_2 entered the mass spectrometer via an open split arrangement within the ConfloIV and were analyzed against their corresponding reference gases. For every ten unknown samples, in-house gelatin standards, which are calibrated to the International Atomic Energy Agency (IAEA) reference materials USGS40 (L-glutamic acid, $\delta^{13}C_{V\text{-}PDB} = -26.39‰$), USGS41 (L-glutamic acid, $\delta^{13}C_{V\text{-}PDB} = +37.63‰$), IAEA-CH-6 (sucrose, $\delta^{13}C_{V\text{-}PDB} = -10.45‰$), USGS25 (ammonium sulfate, $\delta^{15}N_{AIR} = -30.41‰$), IAEA-N-1 (ammonium sulfate, $\delta^{15}N_{AIR} = +0.43‰$) and IAEA-N-2 (ammonium sulfate, $\delta^{15}N_{AIR} = +20.41‰$), were run in duplicate. Results are reported as per mil (‰)

relative to the internationally accepted standards VPDB and AIR, with 1σ precisions of ±0.2‰ and ±0.3‰ for $\delta^{13}C$ and $\delta^{15}N$, respectively.

Following Cook et al. (2015), ^{14}C ages for material whose carbon has derived from both terrestrial and marine sources were corrected using a mixed terrestrial and marine calibration curve that combines the internationally agreed calibration curves of Reimer et al. (2013) for terrestrial/atmospheric samples (IntCal13) with the calibration curve used for marine samples (Marine13). It is a modeled calibration because there is more than one way to determine the percentage of diet that derived from terrestrial/marine resources. As such, the results will vary slightly depending on the method used.

Paired terrestrial-terrestrial and marine-marine ^{14}C measurements from individual contexts were subject to Ward and Wilson (1978) χ^2 tests to evaluate the independent contemporaneity of the samples within each of these two groups (Table 2). Where the pairs from the same context passed the χ^2 test they were considered suitable for use in making the ΔR estimation. Following Russell (2011), ΔR values were calculated for every possible pairing of marine-terrestrial samples within individual contexts. The calculated weighted-mean ΔR was then used in calibration to correct for local reservoir effects from marine carbon.

The Fortran/Unix ΔR calculation program described in Russell (2011) was used for analysis. This program calculates ΔR values through the conversion of the terrestrial ^{14}C measurements to modeled marine ^{14}C age bounds using interpolation between the IntCal13 atmospheric curve and the Marine13 curve (Reimer et al. 2013). The difference between the modeled and the measured marine age is the ΔR value. The 1σ error on the ΔR values is calculated by a propagation of errors as shown in Equation 5.2 in Russell (2011). A weighted-mean ΔR was calculated to provide a single representative value for each context, placing more weight on the values with lower associated errors, as is commonplace in statistical manipulations. An additional weighted-mean of the weighted-mean values was calculated to provide a single representative ΔR value for the Point Barrow area during the Thule period. This ΔR value was then used in calibration to correct for local reservoir effects from marine carbon.

The technique used for Bayesian chronological modeling is a form of Markov Chain Monte Carlo sampling (Buck et al. 1991; 1996) and has been applied using the program OxCal v4.3 (http://c14.arch.ox.ac.uk/). Details of the algorithms employed by OxCal v4.3 are available in Bronk Ramsey (1995; 1998; 2001; 2009) or from the online manual. The fit between the OxCal model and data is gauged with the A_{model} agreement index, with values higher than 60 indicative of good agreement between the model parameters and the dates (Bronk Ramsey 1995). Resulting posterior density estimates from OxCal are calendar years and presented in *italics* as probability ranges with end points rounded outward to the nearest five years. The algorithms used in the models can be derived from the OxCal keywords and bracket structure shown in the probability distribution plot (Figures 1–3). It should be emphasized that the posterior density estimates produced by modeling are not absolute. They are interpretative estimates, which can and will change as further data become available and as other researchers choose to model the existing data from different perspectives.

THE SAMPLES AND MODELS

Coltrain et al. (2016) report AMS ^{14}C and stable isotope measurements from 54 Thule individuals buried in the Nuvuk cemetery. Following the linear dietary model of Arneborg et al. (1999), the percentage of terrestrial protein consumed (with an uncertainty of 10%) was calculated in Coltrain et al. (2016:Table 1) using –12.0‰ and –20.0‰ as $\delta^{13}C$ end members, where –20.0‰ equated to a 100% terrestrial diet, and –12.0‰ represented a 100% marine diet. These dietary estimates are used in the first Bayesian chronological model (Model 1). The second model (Model 2) uses dietary estimates calculated with the same linear equation, but with different $\delta^{13}C$ end members. Specifically, in Model 2 the average $\delta^{13}C$ measured for caribou and seal bones sampled for this study (Table 1) is used to estimate the terrestrial and marine dietary end members, respectively, after adjustment for a trophic level shift of +1‰ (following DeNiro and Epstein 1978). ^{14}C calibrations for this study were corrected using OxCal and 'mixing' the two calibration curves at the calculated percentages for the two different models. Local reservoir effects from marine carbon were corrected with weighted-mean ΔR correction estimated in this study.

The ^{14}C dates from human skeletons were modeled using the prior assumption that they are representative of a single, relatively uniform phase of mortuary activity and have been placed into unordered phases corresponding to their archaeological context. Boundaries were used in OxCal to estimate the start and end date of the overall unordered group.

RESULTS

The measured $\delta^{13}C$ values of the terrestrial mammal bones used within this study (–19.1‰ to –22.8‰), are slightly more enriched when compared to the typical range for animals existing on purely terrestrial dietary resources in C3-dominated environments (e.g. DeNiro and Epstein 1978; Chisholm et al. 1982; Peterson and Fry 1987; Post 2002; Schoeninger and DeNiro 1984) as caribou tend to have more enriched $\delta^{13}C$ values when compared to other herbivores due to seasonal lichen consumption (Britton et al. 2013; Drucker et al. 2010; Fizet et al. 1995).

All terrestrial ^{14}C measurements within paired contexts pass the Ward and Wilson (1978) χ^2 tests, ensuring confidence in the contemporaneity of the terrestrial samples (Table 2). Four of the six pairs of marine ^{14}C measurements within paired contexts pass the Ward and Wilson (1978) χ^2 tests, ensuring confidence in the contemporaneity of those pairs (Table 2). ΔR values from each pairing are shown in Table 2 where they are sorted by the mean terrestrial calibration in each context. These values range from 389 ± 116 years to 535 ± 33 years. Excluding the two contexts that failed χ^2 tests, the weighted-mean value for Point Barrow area during the Thule period is 450 ± 84 years.

The average $\delta^{13}C$ measured for seal and caribou bones sampled for this study is –14.8‰ and –19.6‰, respectively (Table 1). These mean values were adjusted by a trophic level shift of +1‰ (following DeNiro and Epstein 1978) to estimate the terrestrial and marine dietary end members for Model 2 (–13.8‰ and –18.6‰). When compared to the dietary estimates provided by Coltrain et al. (2016), the use of these $\delta^{13}C$ end members results in lower estimates for the percentages of terrestrial protein consumed for the dated human skeletons from the Nuvuk cemetery.

The ^{14}C dates are in good agreement with the Bayesian model assumptions of both models (A_{model}=189.6; A_{model}=178.7). Modeling estimates that mortuary activity related to the directly dated human skeletons at the Nuvuk cemetery began in *cal AD 1000–1370* (*95% probability*; Figure 1; *Model 1: Boundary Start Nuvuk Cemetery*) in Model 1 and *cal AD 1165–1445* (*95% probability*; Figure 1; *Model 2: Boundary Start Nuvuk Cemetery*) in Model 2. This mortuary activity is estimated to have ended in *cal AD 1330–1535* (*95% probability*; Figure 1; *Model 1: Boundary End Nuvuk Cemetery*) in Model 1 and *cal AD 1465–1585* (*95% probability*; Figure 1; *Model 2: Boundary End Nuvuk Cemetery*) in Model 2. The estimated span of this mortuary activity is *80–440 years* (*95% probability*; Figure 3; *Model 1: Span of*

Nuvuk Cemetery) in Model 1 and *75–375 years* (*95% probability*; Figure 3; *Model 2: Span of Nuvuk Cemetery*) in Model 2.

DISCUSSION AND CONCLUSION

This result of this study is three-fold. First, we have used 26 new ^{14}C dates to explore the variation of how the local ΔR value in the Point Barrow region has changed throughout the Thule period (AD 1000–1750) (Table 2), and second, we have modeled dated human skeletons from the Nuvuk cemetery by applying our best ΔR estimate for the Thule period to a Bayesian chronological model to estimate the timing of mortuary activity (Figures 1–4). Third, we have derived end members using local, chronologically relevant samples in a best-fit approach towards estimating the percentage of terrestrial protein consumed in the dated human skeletons and have used these estimates within our chronological modeling.

The results suggest that the local marine reservoir offset varied by approximately 400–500 years throughout the second millennium AD (Table 2). Tentatively, the simplest explanation for these ΔR fluctuations is changes in the annual thawing patterns of Arctic Ocean sea ice. Another source of variability is the fluctuation in the annual discharge of riverine terrigenous carbon into the Beaufort Sea during the spring freshwater runoff (Coltrain et al. 2016). We suggest using our weighted-mean value (450 ± 84 years) as a best-fit local correction for the ^{14}C dating of Thule period (AD 1000–1750) human populations in the Point Barrow area instead of the context-specific ΔR values shown in Table 2, because the sample of individual Thule period ΔR values for Point Barrow (Table 2) is too low to discern a clear temporal relationship (following Russel et al. 2015:40). Our weighted-mean ΔR value (450 ± 84 years) is less than the weighted-mean ΔR value (506 ± 69 years) for Point Barrow in the early 20th century put forth by McNeely et al. (2006), and it may be that global warming from industrialization led to increased melting of Arctic sea ice and the release of old carbon into the early 20th century Arctic oceansphere. However, it is also possible that the early 20th century bivalves collected from Point Barrow dated by McNeely et al. (2006) may have been frozen in place, leading to an overestimate in their ΔR correction.

Thule archaeological studies have yet to adopt the highly innovative new methodologies used by recent North Atlantic archaeological projects for interpreting isotopic data and ^{14}C measurements in Bayesian frameworks to finely trace cultural changes through time (e.g. Cook et al. 2015; Hamilton and Sayle 2018). The combination of stable isotope analysis and chronological modeling in future research should allow for further generational-level insight into cultural and societal changes during the Birnirk to Thule transition. Further, isotopic considerations (e.g. $\delta^{34}S$) and Bayesian mixed modeling methods (Fernandes et al. 2014) should allow for more accurate estimates of the proportion of terrestrial, marine, and freshwater protein in each ^{14}C dated individual; which, could ultimately allow for even more accurate ^{14}C calibrations and Bayesian modeling.

In this case, the application of our ΔR estimates in conjunction with Bayesian chronological modeling has led to an important new finding regarding the timing of the Nuvuk cemetery. Of the two Bayesian chronological models (Figure 4), Model 2 is preferred for interpretation because it utilizes a more accurate reflection of the stable isotope ratios of the human skeletons through using $\delta^{13}C$ end members from fauna that are both geographically and temporally local (Table 1). At *95% probability*, the results of Model 2 show that the mortuary activity in the Nuvuk cemetery related to the directly dated human skeletons began in the early or middle portions of the Thule period and continued for *75–375 years*. Although, it is entirely possible that even earlier burials were present but destroyed from coastal erosion (Jensen 2009a; MacCarthy 1953) and it is feasible that activity at the cemetery began during the Birnirk period (AD 500–1000). In the mid-AD 1900s Wilburt Carter excavated human skeletons at Point Barrow from northern mortuary contexts that had eroded before modern excavations began in the 1990s (Jensen 2009a:25). Even earlier, Captain Rochfort Maguire in HMS Plover spent the winters of 1852 and 1853 in the Elson Lagoon, where he learned from the Iñupiat Eskimos that the ground of Point Barrow had been eroding for generations (Maguire 1988). Maguire noted that people told him that they had been forced to move the village to the location where he encountered them due to erosion at the old site, which they indicated was now underwater. Additionally, two Sicco harpoon heads carved from antler (*Rangifer tarandus*) were recovered from one of the northernmost graves (Nuvuk-01) excavated at Nuvuk (Jensen 2007). Sicco harpoon heads are considered to be Early Thule index fossils (Jensen 2009a:131) and a date from one of these harpoon heads (Beta-180329) has a conventional ^{14}C age of 1110 ± 40 BP (Jensen 2009a:Table 5), calibrating to cal AD 770–1020 (95% confidence). Likewise, while the modeling estimates that mortuary activity related to the directly dated skeletons ceased by *cal AD 1465–1585* (*95% probability*; Figure 1; *Model 2: Boundary End Nuvuk Cemetery*), it is quite possible that mortuary activity at the Nuvuk cemetery continued until the AD 1900s, as surface indications of burials continue along the Nuvuk ridge up to grave markers from the 1920s (Jensen 2009a:208).

There is a great (and so far unexploited) potential to provide a robust and much more accurate chronology for early human colonization and settlement in the Point Barrow region through further applications of Bayesian statistical modeling of ^{14}C measurements corrected with best-fit ΔR values and paleodietary estimates. Moreover, around a dozen archaeological sites in the region contain ample numbers of archaeological contexts with *in situ* faunal remains ideal for archaeological ^{14}C sampling (Ford 1959; Stanford 1976; Hall and Fullerton 1990; Sheehan 1997; Jensen 2009a, 2009b). Ultimately, the Point Barrow chronology will further improve through the continuation of this type of research in the future to address questions about the timing, tempo, and duration of human activity that are of interest to the greater scientific and Native American community.

ACKNOWLEDGEMENTS

Our deep thanks to the Native Village of Barrow Iñupiat Traditional Government, the Ukpeaġvik Iñupiat Corporation, and the Barrow Senior Advisory Council. We would like to further thank Glenn Sheehan, colleagues, and students for excavation of Nuvuk and the other sites sampled for ^{14}C dating. Portions of this research have been funded by the National Science Foundation (Award # OPP-0726253, OPP-1263848, OPP-1355975) and the Carnegie Trust for the Universities of Scotland.

Table 1. New ^{14}C measurements collected for the estimation of ΔR values.							
Laboratory code	**Site**	**Context**	**Material**	**Conventional ^{14}C age (BP)**	**$\delta^{13}C$ (‰)**	**$\delta^{15}N$ (‰)**	**Atomic C:N**
SUERC-68972	Walakpa (49BAR013)	CS 2 Level F (collected 2015).	Likely caribou (*Rangifer tarandus*) long bone	967 ± 29	–19.3	3.1	3.2
SUERC-68973	Walakpa (49BAR013)	CS 2 Level F (collected 2015)	Caribou (*Rangifer tarandus*) rib	1031 ± 27	–20.0	3.3	3.2
SUERC-68977	Walakpa (Utqiaġvik, Alaska)	CS 2 Level F (collected 2015)	Likely ring seal (*Phoca hispida*) radius	1810 ± 29	–14.3	18.5	3.3
SUERC-68978	Walakpa (49BAR013)	CS 2 Level F (collected 2015)	Likely ring seal (*Phoca hispida*) radius	1761 ± 27	–15.1	19.1	3.3
SUERC-68979	Walakpa (49BAR013)	CS 2 Level D (collected 2015)	Likely ring seal (*Phoca hispida*) unfused distal femur end	1637 ± 29	–14.1	18.5	3.2
SUERC-68980	Walakpa (49BAR013)	CS 2 Level D (collected 2015)	Likely ring seal (*Phoca hispida*) tibia	1694 ± 33	–16.8	17.9	3.3
SUERC-68981	Walakpa (49BAR013	CS 2 Level D (collected 2015)	Caribou *(Rangifer tarandus*) long bone fragment	718 ± 24	–20.3	3.4	3.2
SUERC-68982	Walakpa (49BAR013	CS 2 Level D (collected 2015)	Caribou (*Rangifer tarandus*) cranial fragment	710 ± 29	–19.1	5.2	3.2
SUERC-68983	Pingasugruk	SL2: Low Camp (Bucket STWHG)	Likely ring seal (*Phoca hispida*) claw	1084 ± 29	–15.8	18.2	3.5
SUERC-68987	Pingasugruk	SL2: Low Camp (Bucket STWHG)	Likely ring seal (*Phoca hispida*) first phalanx	1285 ± 30	–12.9	19.0	3.2
SUERC-68988	Pingasugruk	SL2: Low Camp (Bucket STWHG)	Caribou (*Rangifer tarandus*) distal radius	376 ± 29	–20.2	3.2	3.4
SUERC-68989	Pingasugruk	SL2: Low Camp (Bucket STWHG)	Caribou (*Rangifer tarandus*) metapodial shaft	374 ± 27	–19.6	3.5	3.2
SUERC-68990	Pingasugruk	SL1: Midden (Tamis RSBQJ)	Caribou (*Rangifer tarandus*) rib fragment	381 ± 29	–19.1	3.4	3.2
SUERC-68991	Pingasugruk	SL1: Midden (Tamis RSBQJ)	Caribou (*Rangifer tarandus*) astragalus	299 ± 27	–19.4	3.0	3.2
SUERC-68992	Pingasugruk	SL1: Midden (Tamis RSBQJ)	Caribou (*Rangifer tarandus*) calcaneus	372 ± 29	–19.4	2.9	3.2
SUERC-68993	Pingasugruk	SL1: Midden (Tamis RSBQJ)	Likely ring seal (*Phoca hispida*) tibia	1265 ± 29	–14.5	19.0	3.3

Table 1. New ^{14}C measurements collected for the estimation of ΔR values.

Laboratory code	Site	Context	Material	Conventional ^{14}C age (BP)	$\delta^{13}C$ (‰)	$\delta^{15}N$ (‰)	Atomic C:N
SUERC-68997	Pingasugruk	SL1: Midden (Tamis RSBQJ)	Likely ring seal (*Phoca hispida*) humerus	1085 ± 29	–15.3	17.0	3.2
SUERC-68998	Pingasugruk	SL1: Midden (Tamis RSBQJ)	Likely ring seal (*Phoca hispida*) femur	1230 ± 27	–15.2	17.3	3.3
SUERC-68999	Pingasugruk	SL2: Kitchen (Bucket LUVYM)	Likely ring seal (*Phoca hispida*) fibula and tibia with tissue	1264 ± 27	–14.4	18.4	3.5
SUERC-69000	Pingasugruk	SL2: Kitchen (Bucket LUVYM)	Likely ring seal (*Phoca hispida*) astragalus	1315 ± 29	–14.4	19.0	3.4
SUERC-69001	Pingasugruk	SL2: Kitchen (Bucket LUVYM)	Caribou (*Rangifer tarandus*) rib fragment	478 ± 33	–20.1	2.9	3.6
SUERC-69002	Pingasugruk	SL2: Kitchen (Bucket LUVYM)	Caribou (*Rangifer tarandus*) mandible fragment with teeth	427 ± 33	–20.0	4.2	3.5
SUERC-69003	Pingasugruk	SL2: Midden (Tamis GUBNN)	Likely ring seal (*Phoca hispida*) femur	1158 ± 29	–15.5	18.7	3.2
SUERC-69007	Pingasugruk	SL2: Midden (Tamis GUBNN)	Likely ring seal (*Phoca hispida*) astragalus	1177 ± 27	–14.6	19.6	3.3
SUERC-69008	Pingasugruk	SL2: Midden (Tamis GUBNN)	Caribou (*Rangifer tarandus*) bone, probable maxilla fragment	388 ± 29	–19.2	2.2	3.2
SUERC-69009	Pingasugruk	SL2: Midden (Tamis GUBNN)	Caribou (*Rangifer tarandus*) distal tibia	321 ± 29	–19.2	2.6	3.2

Table 2. Results of χ^2 testing, calculated dates, and ΔR values for each context.						
Site	**Context**	**Terrestrial χ^2 results**	**Marine χ^2 results**	**Mean terrestrial age (BP)**	**Calibrated range (95% confidence) (cal AD)**	**Weighted-mean ΔR (years)**
Walakpa (49BAR013)	CS 2 Level F	T=2.6; df=1; T'(0.05)=3.8	T=1.5; df=1; T'(0.05)=3.8	1001 ± 20	cal AD 980–1120	390 ± 47
Walakpa (49BAR013)	CS 2 Level D	T=0.0; df=1; T'(0.05)=3.8	T=1.7; df=1; T'(0.05)=3.8	715 ± 19	cal AD 1260–1300	535 ± 33
Pingasugruk	SL2: Kitchen (Bucket LUVYM)	T=1.2; df=1; T'(0.05)=3.8	T=1.7; df=1; T'(0.05)=3.8	453 ± 24	cal AD 1410–1470	386 ± 37
Pingasugruk	SL2: Low Camp (Bucket STWHG)	T=0.0; df=1; T'(0.05)=3.8	T=23.2; df=1; T'(0.05)=3.8	375 ± 20	cal AD 1440–1630	389 ± 116
Pingasugruk	SL2: Midden (Tamis GUBNN)	T=2.7; df=1; T'(0.05)=3.8	T=0.2; df=1; T'(0.05)=3.8	355 ± 21	cal AD 1450–1640	389 ± 116
Pingasugruk	SL1: Midden (Tamis RSBQJ)	T=5.3; df=2; T'(0.05)=6.0	T=21.8; df=2; T'(0.05)=6.0	348 ± 17	cal AD 1460–1640	438 ± 90

FIGURES

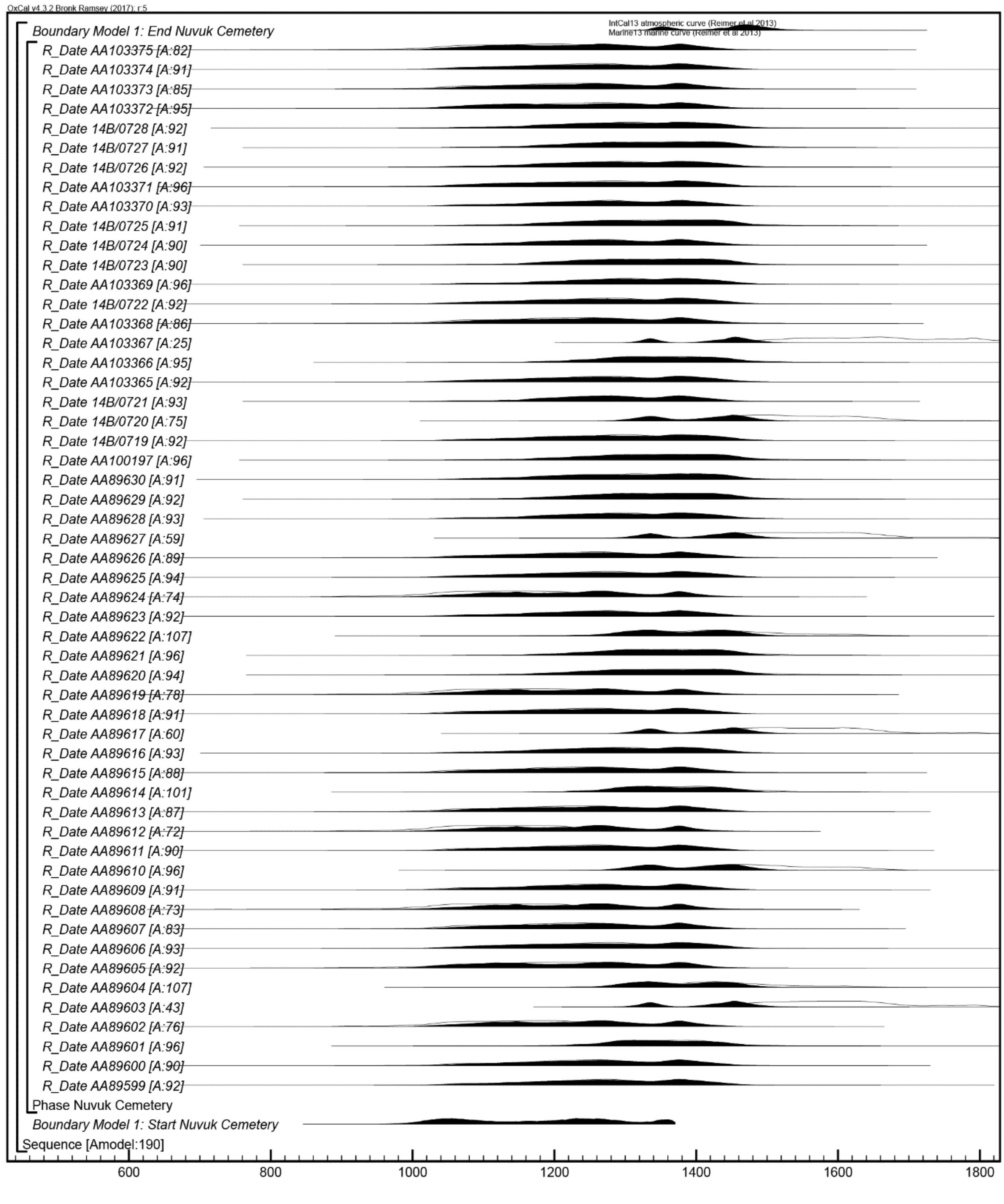

Figure 1. Results and structure of Model 1. The brackets and keywords define the model structure. The outlined distribution is the result of ^{14}C calibration and the solid distributions are the chronological model results. The large square 'brackets' along with the OxCal keywords define the overall model exactly.

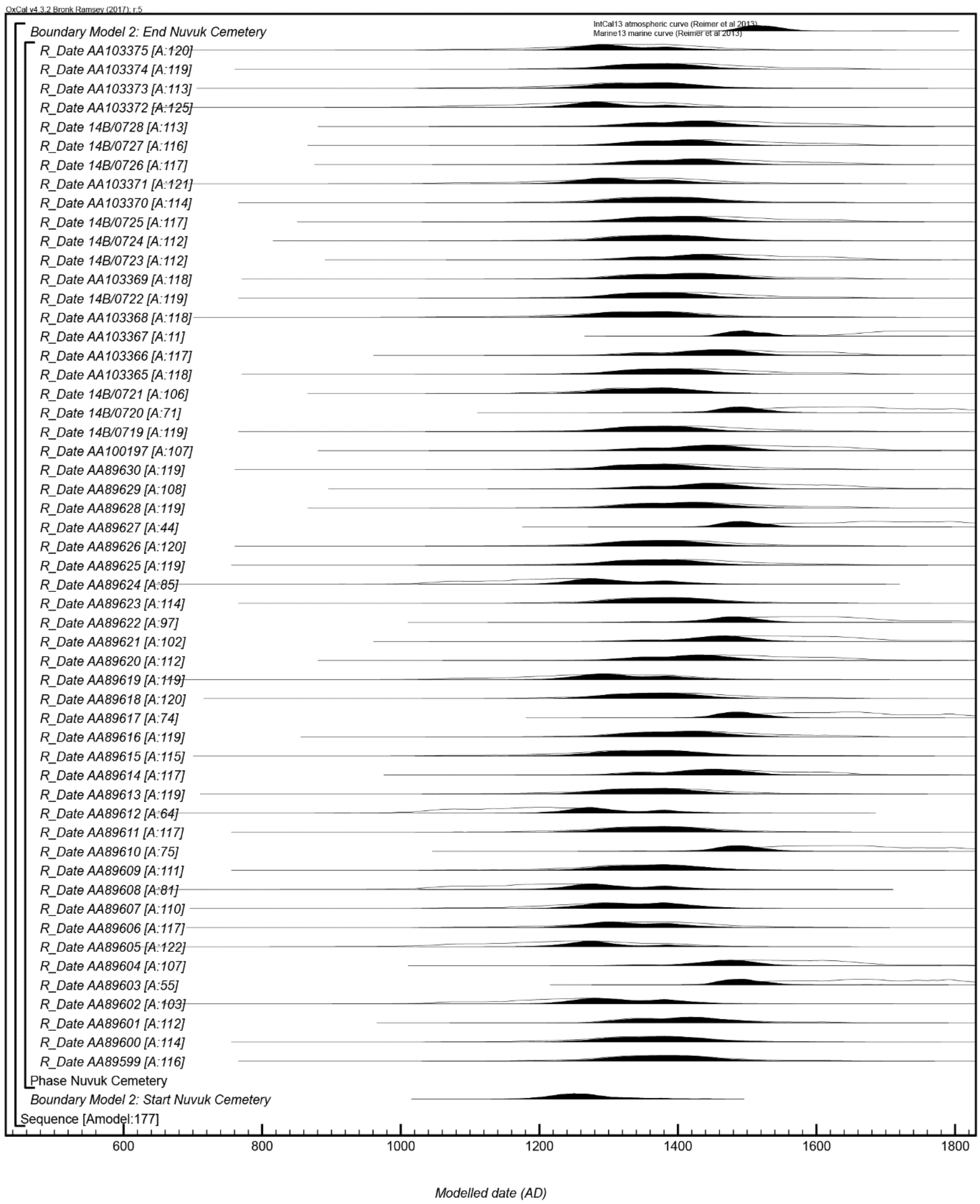

Figure 2. Results and structure of Model 2. The brackets and keywords define the model structure. The format is as described in Figure 1.

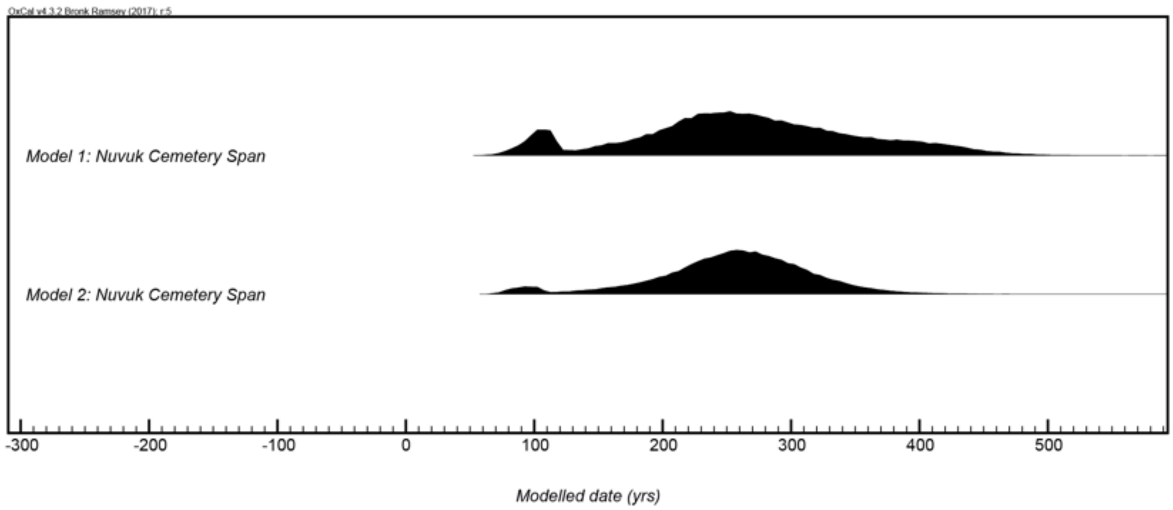

Figure 3. Posterior probabilities for estimated mortuary activity span from the Bayesian models.

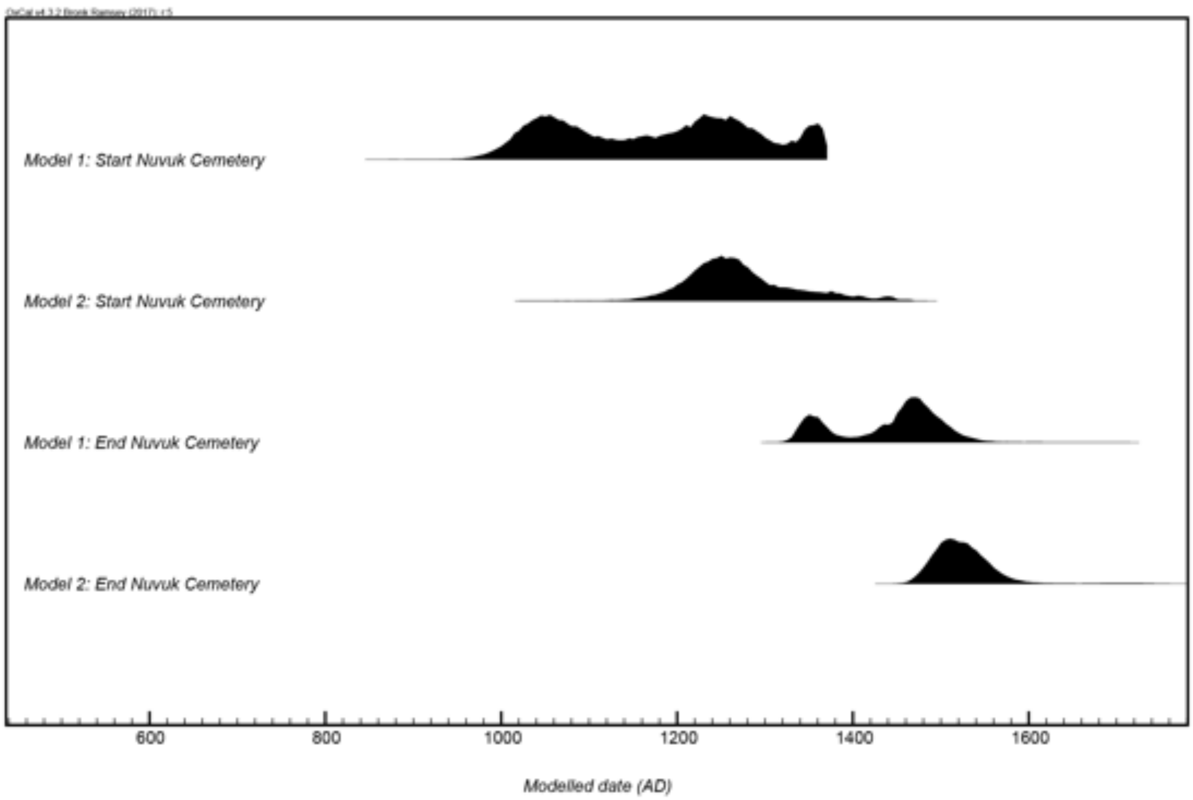

Figure 4. Posterior probability densities derived from Models 1–2 for the starting and ending boundaries for the mortuary activity related to the directly dated human skeletons at the Nuvuk cemetery.

REFERENCES

Arneborg J, Heinemeier J, Lynnerup N, Nielsen HL, Rud N, Sveinbjornsdottir AE. 1999. Change of diet of the Greenland Vikings determined from stable carbon isotope analysis and (super 14) C dating of their bones. Radiocarbon 41(2):157-68.

Ascough PL, Cook GT, Dugmore AJ. 2009. North Atlantic marine 14C reservoir effects: Implications for late-Holocene chronological studies. Quaternary Geochronology 4(3):171-80.

Bayliss A. 2009. Rolling out revolution: using radiocarbon dating in archaeology. Radiocarbon 51(1):123-47.

Bayliss A, Bronk Ramsey C, van der Plicht J, Whittle A. 2007. Bradshaw and Bayes: Towards a Timetable for the Neolithic. Cambridge Archaeological Journal 17(1):1-28.

Bayliss A, van der Plicht J, Bronk Ramsey C, McCormac G, Healy F, Whittle A. 2011. Towards generational time-scales: The quantitative Interpretation of Archaeological Chronologies. In: Whittle A, Healy F, Bayliss A, editors. Gathering Time: Dating the Early Neolithic Enclosures of Southern Britain and Ireland. Oxford: Oxbow Books. p 17-59.

Bengtson JL, Hiruki-Raring LM, Simpkins MA, Boveng PL. 2005. Ringed and bearded seal densities in the eastern Chukchi Sea, 1999–2000. Polar Biology 28(11):833-45.

Britton K, Knecht R, Nehlich O, Hillerdal C, Davis Richard S, Richards Michael P. 2013. Maritime adaptations and dietary variation in prehistoric Western Alaska: Stable isotope analysis of permafrost-preserved human hair. American Journal of Physical Anthropology 151(3):448-61.

Bronk Ramsey C. 1995. Radiocarbon calibration and analysis of stratigraphy: The OxCal program. Radiocarbon 37(2):425-30.

Bronk Ramsey C. 1998. Probability and Dating. Radiocarbon 40(1):461-74.

Bronk Ramsey C. 2001. Development of the radiocarbon calibration program. Radiocarbon 43(2A):355-63.

Bronk Ramsey C. 2009. Bayesian analysis of radiocarbon dates. Radiocarbon 51(1):337-60.

Buck CE, Cavanagh WG, Litton CD. 1996. Bayesian approach to interpreting archaeological data. Chichester: John Wiley & Sons, Ltd.

Buck CE, Kenworthy JB, Litton CD, Smith AFM. 1991. Combining archaeological and radiocarbon information: a Bayesian approach to calibration. Antiquity 65(249):808–21.

Chisholm BS, Nelson DE, Schwarcz HP. 1982. Stable carbon isotope ratios as a measure of marine versus terrestrial protein in ancient diets. Science 216:1131-2.

Coltrain JB, Tackney J, O'Rourke DH. 2016. Thule whaling at Point Barrow, Alaska: The Nuvuk cemetery stable isotope and radiocarbon record. Journal of Archaeological Science: Reports 9:681-94.

Cook GT, Ascough PL, Bonsall C, Hamilton WD, Russell N, Sayle KL, Scott EM, Bownes JM. 2015. Best practice methodology for 14C calibration of marine and mixed terrestrial/marine samples. Quaternary Geochronology 27:164-71.

Crawford JA, Frost KJ, Quakenbush LT, Whiting A. 2012. Different habitat use strategies by subadult and adult ringed seals (Phoca hispida) in the Bering and Chukchi seas. Polar Biology 35(2):241-55.

DeNiro MJ, Epstein S. 1978. Influence of diet on the distribution of carbon isotopes in animals. Geochimica et Cosmochimica Acta 42(5):495-506.

Drucker DG, Hobson KA, Ouellet J-P, Courtois R. 2010. Influence of forage preferences and habitat use on 13C and 15N abundance in wild caribou (Rangifer tarandus caribou) and moose (Alces alces) from Canada. Isotopes in Environmental and Health Studies 46(1):107-21.

Dunbar E, Cook GT, Naysmith P, Tripney BG, Xu S. 2016. AMS 14C Dating at the Scottish Universities Environmental Research Centre (SUERC) Radiocarbon Dating Laboratory. Radiocarbon 58(1):9-23.

Fernandes R, Millard AR, Brabec M, Nadeau M-J, Grootes P. 2014. Food Reconstruction Using Isotopic Transferred Signals (FRUITS): A Bayesian Model for Diet Reconstruction. PLOS ONE 9(2):e87436.
Fizet M, Mariotti A, Bocherens H, Lange-Badré B, Vandermeersch B, Borel JP, Bellon G. 1995. Effect of diet, physiology and climate on carbon and nitrogen stable isotopes of collagen in a late Pleistocene anthropic palaeoecosystem: Marillac, Charente, France. Journal of Archaeological Science 22(1):67-79.
Ford JA. 1959. Eskimo Prehistory in the Vicinity of Point Barrow, Alaska. Anthropological Papers of the American Museum of Natural History and Theory 47(1):1-272.
Hall ES, Fullerton L, editors. 1990. The 1981 Excavations at the Utqiagvik Archaeological Site Barrow, Alaska. Barrow, Alaska: The North Slope Borough Commission on Inupiat History, Language and Culture.
Hamilton WD, Sayle KL. 2018. Stable Isotopes, Chronology, and Bayesian Models for the Viking Archaeology of North-East Iceland. The Journal of Island and Coastal Archaeology:1-11.
Harwood LA, Smith TG, Auld JC. 2012. Fall Migration of Ringed Seals (Phoca hispida) through the Beaufort and Chukchi Seas, 2001–02. Arctic 65(1):35-44.
Jensen AM. 2007. Nuvuk Burial 1: An Early Thule Hunter Of High Status. Alaska Journal of Anthropology 5(1):119-22.
Jensen AM. 2009a. Nuvuk: Point Barrow, Alaska: The Thule Cemetery and Ipiutak Occupation [PhD Dissertation]: Bryn Mawr College.
Jensen AM. 2009b. Radiocarbon Dates from Recent Excavations at Nuvuk, Point Barrow, Alaska and Their Implications for Neoeskimo Prehistory. On the Track of the Thule Culture From Bering Strait to East Greenland. Copenhagen: National Museum of Denmark, SILA. p 45-62.
Jensen AM. 2014. The Archaeology of North Alaska: Point Hope in Context. In: Auerbach B, Hilton C, Cowgil L, editors. The Foragers of Point Hope: The Biology and Archaeology of Humans on the Edge of the Alaskan Arctic: Cambridge University Press. p 11–34.
Kelly BP, Badajos OH, Kunnasranta M, Moran JR, Martinez-Bakker M, Wartzok D, Boveng P. 2010. Seasonal home ranges and fidelity to breeding sites among ringed seals. Polar Biology 33(8):1095-109.
Krafft BA, Kovacs KM, Lydersen C. 2007. Distribution of sex and age groups of ringed seals Pusa hispida in the fast-ice breeding habitat of Kongsfjorden, Svalbard. Marine Ecology Progress Series 335:199-206.
Lowry LF, Frost KJ, Davis R, DeMaster DP, Suydam RS. 1998. Movements and behavior of satellite-tagged spotted seals (Phoca largha) in the Bering and Chukchi Seas. Polar Biology 19(4):221-30.
MacCarthy GR. 1953. Recent Changes in the Shoreline near Point Barrow, Alaska. Arctic 6(1):44-51.
Maguire R, Captain. 1988. The Journal of Rochfort Maguire, 1852-1854: Two Years at Point Barrow, Alaska, Aboard HMS Plover in the search for Sir John Franklin. London: The Hakluyt Society.
Masters PM. 1987. Preferential preservation of non-collagenous protein during bone diagenesis: implications for chronometric ad stable isotope measurements. Geochimica et Cosmochimica Acta 51:3209-14.
Maxwell MS. 1985. Prehistory of the Eastern Arctic. Orlando, Florida: Academic.
McGhee R. 1996. Ancient People of the Arctic. Vancouver: University of British Columbia Press.
McGhee R. 2009. When and why did the Inuit move to the eastern Arctic. In: Maschner H, Mason O, McGhee R, editors. The Northern World, AD 900–1400. Salt Lake City: University of Utah Press. p 155-63.
McNeely R, Dyke AS, Southon JR. 2006. Canadian marine reservoir ages, preliminary data assessment. Geological Survey Canada.

Morrison DA. 2009. The "Arctic Maritime" Expansion: A View from the Western Canadian Arctic. In: Maschner HDG, Mason OK, McGhee R, editors. The Dynamics of Climate, Economy, and Politics in Hemispheric Perspective. Salt Lake City: University of Utah Press. p 164-78.
Naysmith P, Cook G, Freeman S, Scott EM, Anderson R, Dunbar E, Muir G, Dougans A, Wilcken K, Schnabel C, Russell N, Ascough P, Maden C. 2010. 14C AMS at SUERC: improving QA data from the 5 MV tandem AMS and 250 kV SSAMS. Radiocarbon 52(2):263-71.
Peterson BJ, Fry B. 1987. Stable Isotopes in Ecosystem Studies. Annual Review of Ecology and Systematics 18(1):293-320.
Post DM. 2002. Using Stable Isotopes to Estimate Trophic Position: Models, Methods, and Assumptions. Ecology 83(3):703-18.
Queiroz-Alves E, Kita M, Philippa A, Christopher Bronk R. 2018. The Worldwide Marine Radiocarbon Reservoir Effect: Definitions, Mechanisms, and Prospects. Reviews of Geophysics 56(1):278-305.
Raghavan M, DeGiorgio M, Albrechtsen A, Moltke I, Skoglund P, Korneliussen TS, Grønnow B, Appelt M, Gulløv HC, Friesen TM, Fitzhugh W, Malmström H, Rasmussen S, Olsen J, Melchior L, Fuller BT, Fahrni SM, Stafford T, Grimes V, Renouf MAP, Cybulski J, Lynnerup N, Lahr MM, Britton K, Knecht R, Arneborg J, Metspalu M, Cornejo OE, Malaspinas A-S, Wang Y, Rasmussen M, Raghavan V, Hansen TVO, Khusnutdinova E, Pierre T, Dneprovsky K, Andreasen C, Lange H, Hayes MG, Coltrain J, Spitsyn VA, Götherström A, Orlando L, Kivisild T, Villems R, Crawford MH, Nielsen FC, Dissing J, Heinemeier J, Meldgaard M, Bustamante C, O'Rourke DH, Jakobsson M, Gilbert MTP, Nielsen R, Willerslev E. 2014. The genetic prehistory of the New World Arctic. Science 345(6200).
Reimer PJ, Bard E, Bayliss A, Beck JW, Blackwell PG, Ramsey CB, Buck CE, Cheng H, Edwards RL, Friedrich M, Grootes PM, Guilderson TP, Haflidason H, Hajdas I, Hatté C, Heaton TJ, Hoffmann DL, Hogg AG, Hughen KA, Kaiser KF, Kromer B, Manning SW, Niu M, Reimer RW, Richards DA, Scott EM, Southon JR, Staff RA, Turney CSM, van der Plicht J. 2013. IntCal13 and Marine13 Radiocarbon Age Calibration Curves 0–50,000 Years cal BP. Radiocarbon 55(4):1869-87.
Russell N. 2011. Marine Radiocarbon Reservoir Effects (MRE) in Archaeology: Temporal and Spatial Changes through the Holocene within the UK Coastal Environment [PhD Dissertation]: University of Glasgow.
Russell N, Cook GT, Ascough PL, Dugmore AJ. 2010. Spatial Variation in the Marine Radiocarbon Reservoir Effect Throughout the Scottish Post-Roman to Late Medieval Period: North Sea Values (500–1350 BP). Radiocarbon 52(3):1166-81.
Russell N, Cook GT, Ascough PL, Scott EM. 2015. A period of calm in Scottish seas: A comprehensive study of ΔR values for the northern British Isles coast and the consequent implications for archaeology and oceanography. Quaternary Geochronology 30:34-41.
Schoeninger MJ, DeNiro MJ. 1984. Nitrogen and carbon isotopic composition of bone collagen from marine and terrestrial animals. Geochimica et Cosmochimica Acta 48(4):625-39.
Scott EM. 2003. The Third International Radiocarbon Intercomparison (TIRI) and the Fourth International Radiocarbon Intercomparison (FIRI) 1990-2002: results, analysis, and conclusions. Radiocarbon 45(2):135-408.
Scott EM, Bryant C, Cook GT, Naysmith P. 2003. Is there a fifth international radiocarbon intercomparison (VIRI)? Radiocarbon 45:493-5.
Scott EM, Cook GT, Naysmith P. 2010. A report on phase 2 of the Fifth International Radiocarbon Intercomparison (VIRI). Radiocarbon 52(3):846-58.
Scott EM, Cook GT, Naysmith P, Bryant C, O'Donnell D. 2007. A report on phase 1 of the 5th international radiocarbon intercomparison (VIRI). Radiocarbon 49:409-26.
Sheehan G. 1997. In the belly of the whale: trade and war in Eskimo society. Anchorage: Alaska Anthropological Association.

Stanford D. 1976. The Walakpa Site, Alaska: Its Place in the Birnirk and Thule Cultures. Washington, D.C.: Smithsonian Institution Press.
Stuiver M, Kra RS. 1986. Editorial comment. Radiocarbon 28(2B):ii.
Stuiver M, Polach HA. 1977. Reporting of 14C data. Radiocarbon 19(3):355-63.
Tuross N, Fogel ML, Hare PE. 1988. Variability in the preservation of the isotopic composition of collagen from fossil bone. Geochimica et Cosmochimica Acta 52:929-35.
Ward GK, Wilson SR. 1978. Procedures for Comparing and Combining Radiocarbon Age-Determinations: A Critique. Archaeometry 20(1):19-31.

SUPPLEMENTAL MATERIAL: OXCAL CODE

MODEL 1:

```
Plot()
 {
  Sequence()
  {
   Boundary("Model 1: Start Nuvuk Cemetery");
   Phase("Nuvuk Cemetery")
   {
    Curve("IntCal13","IntCal13.14c");
    Curve("Marine13","Marine13.14c");
    Delta_R("LocalMarine",450 ,84);
    Mix_Curve("Mixed","IntCal13","LocalMarine",70.2,10);
    R_Date("AA89599", 1318, 37);
    Mix_Curve("Mixed","IntCal13","LocalMarine",69,10);
    R_Date("AA89600", 1331, 41);
    Mix_Curve("Mixed","IntCal13","LocalMarine",54.8,10);
    R_Date("AA89601", 1051, 34);
    Mix_Curve("Mixed","IntCal13","LocalMarine",65.4,10);
    R_Date("AA89602", 1401, 34);
    Mix_Curve("Mixed","IntCal13","LocalMarine",60.3,10);
    R_Date("AA89603", 823, 33);
    Mix_Curve("Mixed","IntCal13","LocalMarine",68,10);
    R_Date("AA89604", 1085, 37);
    Mix_Curve("Mixed","IntCal13","LocalMarine",92.6,10);
    R_Date("AA89605", 1586, 41);
    Mix_Curve("Mixed","IntCal13","LocalMarine",88,10);
    R_Date("AA89606", 1460, 35);
    Mix_Curve("Mixed","IntCal13","LocalMarine",63.8,10);
    R_Date("AA89607", 1328, 35);
    Mix_Curve("Mixed","IntCal13","LocalMarine",59.9,10);
    R_Date("AA89608", 1380, 35);
    Mix_Curve("Mixed","IntCal13","LocalMarine",65,10);
    R_Date("AA89609", 1292, 43);
    Mix_Curve("Mixed","IntCal13","LocalMarine",74.9,10);
    R_Date("AA89610", 1081, 39);
    Mix_Curve("Mixed","IntCal13","LocalMarine",71.5,10);
    R_Date("AA89611", 1354, 40);
    Mix_Curve("Mixed","IntCal13","LocalMarine",53.5,10);
```

```
R_Date("AA89612", 1326, 35);
Mix_Curve("Mixed","IntCal13","LocalMarine",74.9,10);
R_Date("AA89613", 1407, 41);
Mix_Curve("Mixed","IntCal13","LocalMarine",63.1,10);
R_Date("AA89614", 1092, 40);
Mix_Curve("Mixed","IntCal13","LocalMarine",69.3,10);
R_Date("AA89615", 1353, 45);
Mix_Curve("Mixed","IntCal13","LocalMarine",74.3,10);
R_Date("AA89616", 1311, 35);
Mix_Curve("Mixed","IntCal13","LocalMarine",62.2,10);
R_Date("AA89617", 894, 34);
Mix_Curve("Mixed","IntCal13","LocalMarine",76.3,10);
R_Date("AA89618", 1398, 49);
Mix_Curve("Mixed","IntCal13","LocalMarine",72.8,10);
R_Date("AA89619", 1463, 35);
Mix_Curve("Mixed","IntCal13","LocalMarine",84.9,10);
R_Date("AA89620", 1310, 36);
Mix_Curve("Mixed","IntCal13","LocalMarine",76.9,10);
R_Date("AA89621", 1239, 43);
Mix_Curve("Mixed","IntCal13","LocalMarine",73.6,10);
R_Date("AA89622", 1130, 44);
Mix_Curve("Mixed","IntCal13","LocalMarine",68.6,10);
R_Date("AA89623", 1299, 35);
Mix_Curve("Mixed","IntCal13","LocalMarine",61.6,10);
R_Date("AA89624", 1390, 34);
Mix_Curve("Mixed","IntCal13","LocalMarine",80.3,10);
R_Date("AA89625", 1397, 46);
Mix_Curve("Mixed","IntCal13","LocalMarine",74.7,10);
R_Date("AA89626", 1377, 34);
Mix_Curve("Mixed","IntCal13","LocalMarine",71.3,10);
R_Date("AA89627", 963, 41);
Mix_Curve("Mixed","IntCal13","LocalMarine",73.1,10);
R_Date("AA89628", 1295, 34);
Mix_Curve("Mixed","IntCal13","LocalMarine",78.9,10);
R_Date("AA89629", 1282, 34);
Mix_Curve("Mixed","IntCal13","LocalMarine",89.4,10);
R_Date("AA89630", 1402, 33);
Mix_Curve("Mixed","IntCal13","LocalMarine",80.1,10);
R_Date("AA100197", 1280, 50);
Mix_Curve("Mixed","IntCal13","LocalMarine",84,10);
R_Date("14B/0719", 1390, 30);
Mix_Curve("Mixed","IntCal13","LocalMarine",83.9,10);
R_Date("14B/0720", 1110, 20);
Mix_Curve("Mixed","IntCal13","LocalMarine",57.5,10);
R_Date("14B/0721", 1190, 20);
Mix_Curve("Mixed","IntCal13","LocalMarine",77.1,10);
R_Date("AA103365", 1370, 39);
Mix_Curve("Mixed","IntCal13","LocalMarine",68.5,10);
R_Date("AA103366", 1171, 39);
Mix_Curve("Mixed","IntCal13","LocalMarine",66.2,10);
R_Date("AA103367", 803, 38);
Mix_Curve("Mixed","IntCal13","LocalMarine",72.9,10);
```

```
   R_Date("AA103368", 1399, 40);
   Mix_Curve("Mixed","IntCal13","LocalMarine",80.2,10);
   R_Date("14B/0722", 1390, 30);
   Mix_Curve("Mixed","IntCal13","LocalMarine",69.1,10);
   R_Date("AA103369", 1246, 58);
   Mix_Curve("Mixed","IntCal13","LocalMarine",80.4,10);
   R_Date("14B/0723", 1310, 20);
   Mix_Curve("Mixed","IntCal13","LocalMarine",66.9,10);
   R_Date("14B/0724", 1290, 20);
   Mix_Curve("Mixed","IntCal13","LocalMarine",85.8,10);
   R_Date("14B/0725", 1350, 30);
   Mix_Curve("Mixed","IntCal13","LocalMarine",69.3,10);
   R_Date("AA103370", 1300, 39);
   Mix_Curve("Mixed","IntCal13","LocalMarine",91.4,10);
   R_Date("AA103371", 1484, 52);
   Mix_Curve("Mixed","IntCal13","LocalMarine",75.9,10);
   R_Date("14B/0726", 1320, 30);
   Mix_Curve("Mixed","IntCal13","LocalMarine",85.7,10);
   R_Date("14B/0727", 1340, 30);
   Mix_Curve("Mixed","IntCal13","LocalMarine",78,10);
   R_Date("14B/0728", 1320, 30);
   Mix_Curve("Mixed","IntCal13","LocalMarine",95.2,10);
   R_Date("AA103372", 1539, 44);
   Mix_Curve("Mixed","IntCal13","LocalMarine",67.1,10);
   R_Date("AA103373", 1347, 39);
   Mix_Curve("Mixed","IntCal13","LocalMarine",77.5,10);
   R_Date("AA103374", 1395, 39);
   Mix_Curve("Mixed","IntCal13","LocalMarine",78.8,10);
   R_Date("AA103375", 1493, 40);
  };
  Boundary("Model 1: End Nuvuk Cemetery");
  Span("Nuvuk Cemetery Span");
 };
};
```

MODEL 2:

```
Plot()
 {
 Sequence()
  {
  Boundary("Model 2: Start Nuvuk Cemetery");
  Phase("Nuvuk Cemetery")
   {
   Curve("IntCal13","IntCal13.14c");
   Curve("Marine13","Marine13.14c");
   Delta_R("LocalMarine",450 ,84);
   Mix_Curve("Mixed","IntCal13","LocalMarine",87.5,10);
   R_Date("AA89599", 1318, 37);
   Mix_Curve("Mixed","IntCal13","LocalMarine",85.4,10);
   R_Date("AA89600", 1331, 41);
   Mix_Curve("Mixed","IntCal13","LocalMarine",62.5,10);
```

```
R_Date("AA89601", 1051, 34);
Mix_Curve("Mixed","IntCal13","LocalMarine",79.2,10);
R_Date("AA89602", 1401, 34);
Mix_Curve("Mixed","IntCal13","LocalMarine",70.8,10);
R_Date("AA89603", 823, 33);
Mix_Curve("Mixed","IntCal13","LocalMarine",83.3,10);
R_Date("AA89604", 1085, 37);
Mix_Curve("Mixed","IntCal13","LocalMarine",100,10);
R_Date("AA89605", 1586, 41);
Mix_Curve("Mixed","IntCal13","LocalMarine",100,10);
R_Date("AA89606", 1460, 35);
Mix_Curve("Mixed","IntCal13","LocalMarine",77.1,10);
R_Date("AA89607", 1328, 35);
Mix_Curve("Mixed","IntCal13","LocalMarine",70.8,10);
R_Date("AA89608", 1380, 35);
Mix_Curve("Mixed","IntCal13","LocalMarine",79.2,10);
R_Date("AA89609", 1292, 43);
Mix_Curve("Mixed","IntCal13","LocalMarine",95.8,10);
R_Date("AA89610", 1081, 39);
Mix_Curve("Mixed","IntCal13","LocalMarine",89.6,10);
R_Date("AA89611", 1354, 40);
Mix_Curve("Mixed","IntCal13","LocalMarine",60.4,10);
R_Date("AA89612", 1326, 35);
Mix_Curve("Mixed","IntCal13","LocalMarine",95.8,10);
R_Date("AA89613", 1407, 41);
Mix_Curve("Mixed","IntCal13","LocalMarine",75,10);
R_Date("AA89614", 1092, 40);
Mix_Curve("Mixed","IntCal13","LocalMarine",85.4,10);
R_Date("AA89615", 1353, 45);
Mix_Curve("Mixed","IntCal13","LocalMarine",93.8,10);
R_Date("AA89616", 1311, 35);
Mix_Curve("Mixed","IntCal13","LocalMarine",75,10);
R_Date("AA89617", 894, 34);
Mix_Curve("Mixed","IntCal13","LocalMarine",97.9,10);
R_Date("AA89618", 1398, 49);
Mix_Curve("Mixed","IntCal13","LocalMarine",91.7,10);
R_Date("AA89619", 1463, 35);
Mix_Curve("Mixed","IntCal13","LocalMarine",100,10);
R_Date("AA89620", 1310, 36);
Mix_Curve("Mixed","IntCal13","LocalMarine",100,10);
R_Date("AA89621", 1239, 43);
Mix_Curve("Mixed","IntCal13","LocalMarine",93.8,10);
R_Date("AA89622", 1130, 44);
Mix_Curve("Mixed","IntCal13","LocalMarine",85.4,10);
R_Date("AA89623", 1299, 35);
Mix_Curve("Mixed","IntCal13","LocalMarine",72.9,10);
R_Date("AA89624", 1390, 34);
Mix_Curve("Mixed","IntCal13","LocalMarine",100,10);
R_Date("AA89625", 1397, 46);
Mix_Curve("Mixed","IntCal13","LocalMarine",95.8,10);
R_Date("AA89626", 1377, 34);
Mix_Curve("Mixed","IntCal13","LocalMarine",89.6,10);
```

```
 R_Date("AA89627", 963, 41);
 Mix_Curve("Mixed","IntCal13","LocalMarine",91.7,10);
 R_Date("AA89628", 1295, 34);
 Mix_Curve("Mixed","IntCal13","LocalMarine",100,10);
 R_Date("AA89629", 1282, 34);
 Mix_Curve("Mixed","IntCal13","LocalMarine",100,10);
 R_Date("AA89630", 1402, 33);
 Mix_Curve("Mixed","IntCal13","LocalMarine",100,10);
 R_Date("AA100197", 1280, 50);
 Mix_Curve("Mixed","IntCal13","LocalMarine",100,10);
 R_Date("14B/0719", 1390, 30);
 Mix_Curve("Mixed","IntCal13","LocalMarine",100,10);
 R_Date("14B/0720", 1110, 20);
 Mix_Curve("Mixed","IntCal13","LocalMarine",66.7,10);
 R_Date("14B/0721", 1190, 20);
 Mix_Curve("Mixed","IntCal13","LocalMarine",100,10);
 R_Date("AA103365", 1370, 39);
 Mix_Curve("Mixed","IntCal13","LocalMarine",85.4,10);
 R_Date("AA103366", 1171, 39);
 Mix_Curve("Mixed","IntCal13","LocalMarine",81.3,10);
 R_Date("AA103367", 803, 38);
 Mix_Curve("Mixed","IntCal13","LocalMarine",91.7,10);
 R_Date("AA103368", 1399, 40);
 Mix_Curve("Mixed","IntCal13","LocalMarine",100,10);
 R_Date("14B/0722", 1390, 30);
 Mix_Curve("Mixed","IntCal13","LocalMarine",85.4,10);
 R_Date("AA103369", 1246, 58);
 Mix_Curve("Mixed","IntCal13","LocalMarine",100,10);
 R_Date("14B/0723", 1310, 20);
 Mix_Curve("Mixed","IntCal13","LocalMarine",83.3,10);
 R_Date("14B/0724", 1290, 20);
 Mix_Curve("Mixed","IntCal13","LocalMarine",100,10);
 R_Date("14B/0725", 1350, 30);
 Mix_Curve("Mixed","IntCal13","LocalMarine",85.4,10);
 R_Date("AA103370", 1300, 39);
 Mix_Curve("Mixed","IntCal13","LocalMarine",100,10);
 R_Date("AA103371", 1484, 52);
 Mix_Curve("Mixed","IntCal13","LocalMarine",97.9,10);
 R_Date("14B/0726", 1320, 30);
 Mix_Curve("Mixed","IntCal13","LocalMarine",100,10);
 R_Date("14B/0727", 1340, 30);
 Mix_Curve("Mixed","IntCal13","LocalMarine",100,10);
 R_Date("14B/0728", 1320, 30);
 Mix_Curve("Mixed","IntCal13","LocalMarine",100,10);
 R_Date("AA103372", 1539, 44);
 Mix_Curve("Mixed","IntCal13","LocalMarine",83.3,10);
 R_Date("AA103373", 1347, 39);
 Mix_Curve("Mixed","IntCal13","LocalMarine",100,10);
 R_Date("AA103374", 1395, 39);
 Mix_Curve("Mixed","IntCal13","LocalMarine",100,10);
 R_Date("AA103375", 1493, 40);
};
```

```
  Boundary("Model 2: End Nuvuk Cemetery");
  Span("Nuvuk Cemetery Span");
 };
};
```